AIMS Geosciences

AIMS Geosciences, 3 (3): 304-326
DOI: 10.3934/geosci.2017.3.304
Received date 19 February 2017
Accepted date 05 July 2017
Published date 10 July 2017

http://www.aimspress.com/journal/geosciences

Research article

Observations of the Hawaiian Mesopelagic Boundary Community in Daytime and Nighttime Habitats Using Estimated Backscatter

Comfort CM [1,*], Smith KA [1], McManus MA [1], Neuheimer AB [1], Sevadjian JC [2] and Ostrander CE [3]

[1] Department of Oceanography, University of Hawaii at Manoa, 1000 Pope Rd, Honolulu, HI 96822
[2] Monterey Bay Aquarium Research Institute, 7700 Sandholdt Rd, Moss Landing, CA 95039
[3] School of Ocean and Earth Science and Technology, 1680 East West Rd, University of Hawaii at Manoa, Honolulu, HI 96822

* **Correspondence:** ccomfort@hawaii.edu.

Abstract: The Hawaiian mesopelagic boundary community is a slope-associated assemblage of micronekton that undergoes diel migrations along the slopes of the islands, residing at greater depths during the day and moving upslope to forage in shallower water at night. The timing of these migrations may be influenced by environmental factors such as moon phase or ambient light. To investigate the movements of this community, we examined echo intensity data from acoustic Doppler current profilers (ADCPs) deployed at shallow and deep sites on the southern slope of Oahu, Hawaii. Diel changes in echo intensity (and therefore in estimated backscatter) were observed and determined to be caused, at least in part, by the horizontal migration of the mesopelagic boundary community. Generalized additive modeling (GAM) was used to assess the impact of environmental factors on the migration timing. Sunset time and lunar illumination were found to be significant factors. Movement speeds of the mesopelagic boundary community were

estimated at 1.25–1.99 km h^{-1} (35–55 cm s^{-1}). The location at which the migrations were observed is the future site of a seawater air conditioning system, which will cause artificial upwelling at our shallow observation site and may cause animal entrainment at the seawater intake near our deep water observation site. This study is the first to observe the diel migration of the mesopelagic boundary community on southern Oahu in both deep and shallow parts of the habitat, and it is also the first to examine migration trends over long time scales, which allows a better assessment of the effects of seasons and lunar illumination on micronekton migrations. Understanding the driving mechanisms of mesopelagic boundary community behavior will increase our ability to assess and manage coastal ecosystems in the face of increasing anthropogenic impacts.

Keywords: Mesopelagic boundary community; diel migration; mesopelagic micronekton; Hawaiian Islands; slope habitat

1. Introduction

Diel migrations are a common behavior pattern in a wide variety of marine species, from zooplankton to apex predators. Throughout the world's oceans, many micronekton undertake diel vertical migrations, coming to shallower, near-surface waters at night to forage, and retreating to deeper, darker waters during the day to avoid visual predators [1–3]. Some micronekton may also focus their spawning in the warmer, shallower portion of their diel migration [4,5]. The timing of vertical migrations and the related changes in bulk acoustic backscatter are correlated with times of sunset and sunrise [3], and micronekton have been shown to adjust their depth to stay within a preferred range of light intensity [6].

Near the slopes of islands and seamounts, some micronekton associate with the benthos throughout their diel migrations [7,8], resulting in longer migrations because there is an added horizontal travel component [9]. In the Hawaiian Islands, this layer has been termed the "mesopelagic boundary community," and organisms in this slope-associated community include micronektonic fish, squid, and shrimp [7,9]. The majority of this community is made up of multiple species of myctophid fishes [9]. Observations of organism density by stereo-video camera have shown a maximum density of 1,800 organisms m^{-3} on western Oahu and 700 organisms m^{-3} on the Big Island of Hawaii, with averages of 15–23 organisms m^{-3} [9]. These organisms are a key trophic link between zooplankton and larger predators in slope ecosystems [10], and due to their significant horizontal migrations, they may also facilitate nutrient transport between different regions of the slope. The diel migrations of this slope-associated community may be influenced by the amount of light in the water column, as has been observed in pelagic zooplankton and micronekton vertical migrations elsewhere in the world [6,11–13].

As the Hawaiian mesopelagic boundary community undertakes these daily migrations along

the slope of the islands, the community travels from depths of > 400 m in the daytime to as shallow as 10–100 m during the night [7,14]. The distance of this migration depends on the steepness of the island slope, but round-trips of up to 11 km have been observed on the western slope of Oahu, Hawaii [9]. Moon phase, but not sunset time, has previously been found to correlate with arrival time of the mesopelagic boundary community in the shallow nighttime habitat [15]. If light-mediated visual predation is an important factor driving migrations, it follows that smaller organisms should arrive before larger ones since they are harder to see [9]. However, larger organisms have actually been observed arriving before smaller organisms [9], indicating that the faster swimming speed of larger organisms may be more important than avoidance of light. Overall, the relationship of water-column light to mesopelagic boundary community horizontal migration timing is unclear.

In this contribution, we present novel observations of the migration of the mesopelagic boundary community between the daytime and nighttime habitats on the southern slope of Oahu, Hawaii, in the region of a proposed seawater air conditioning system. We investigate the hypothesis that ambient light is an important factor in the timing of mesopelagic boundary layer migrations. Additionally, we demonstrate how the estimated backscatter data from uncalibrated ADCPs can be useful to investigate biological questions regarding behavior of the mesopelagic sound scattering community.

2. Methods

2.1. Study site

The study area was offshore of Honolulu, Oahu, Hawaii, USA. Mamala Bay is an open embayment spanning from Barber's Point (21.29 °N, 158.11 °W) to Diamond Head (21.25 °N, 157.81 °W). Moorings were deployed in an area within Mamala Bay at approximately 21.28 °N and 157.87 °W and an area outside Mamala Bay near 21.24 °N and 157.89 °W. The instruments were deployed for multiple periods between March 1, 2013 and November 7, 2016.

2.2. Field deployments

ADCPs were deployed between March 2013 and November 2016 (Figure 1; S1–S8) as part of an ongoing environmental assessment for a proposed seawater air conditioning plant [20] and one ADCP was deployed in a separate physical oceanography study further offshore (Table 1). The shallow deployments were within Mamala Bay about 1.7 km from shore. For these eight shallow deployments, an upward-looking 300 kHz ADCP was situated in a frame on the seafloor. These deployments occurred sequentially in time (Table 1). The deployments were between 106–152 m, within the deeper part of the typical nighttime residence depth of the mesopelagic boundary community [9].

Table 1. Instrumentation, depths, locations, and deployment dates of 300 kHz ADCPs.

Mooring ID	*Water depth (m)*	*Instrument*	*Instrument depth (m)*	*Orientation*	*Latitude (°N)*	*Longitude (°W)*	*Deployed*	*Recovered*
S1	120	RDI Workhorse	119	Up	21.2802	157.8721	04/22/13	07/10/13
S2	145	RDI Workhorse	144	Up	21.2791	157.8722	08/06/13	10/14/13
S3	130	RDI Sentinel V	129	Up	21.2797	157.8723	04/24/14	07/25/14
S4	152	RDI Sentinel V	151	Up	21.2790	157.8720	04/20/15	07/23/15
S5	106	RDI Sentinel V	105	Up	212793	157.8698	08/18/15	11/19/15
S6	127	RDI Sentinel V	127	Up	21.2791	157.8713	12/11/15	03/18/16
S7	120	RDI Sentinel V	119	Up	21.2791	157.8713	04/14/16	07/11/16
S8	150	RDI Sentinel V	149	Up	27.2792	157.8719	07/18/16	11/07/16
D	517	RDI Workhorse	426	Down	21.2353	157.8896	03/01/13	08/30/13

One instrument was deployed downslope, outside Mamala Bay and about 6.8 km from shore. The downslope deployment (Figure 1, D) was located within the daytime residence depths of the mesopelagic boundary community; here, a downward-looking 300 kHz ADCP was moored 91 m above bottom in a water depth of 517 m. The deep ADCP was deployed from March 2013 through August 2013 (Table 1).

For the shallow deployments, the ADCPs sampled at a ping rate of 12 s and data were averaged over 10-min intervals and 4 m depth bins. For the deep deployment, the ADCP sampled at a ping rate of 4.8 s and data were averaged over 2 min intervals and 2 m depth bins. For all deployments, the profiling range was ~100 m.

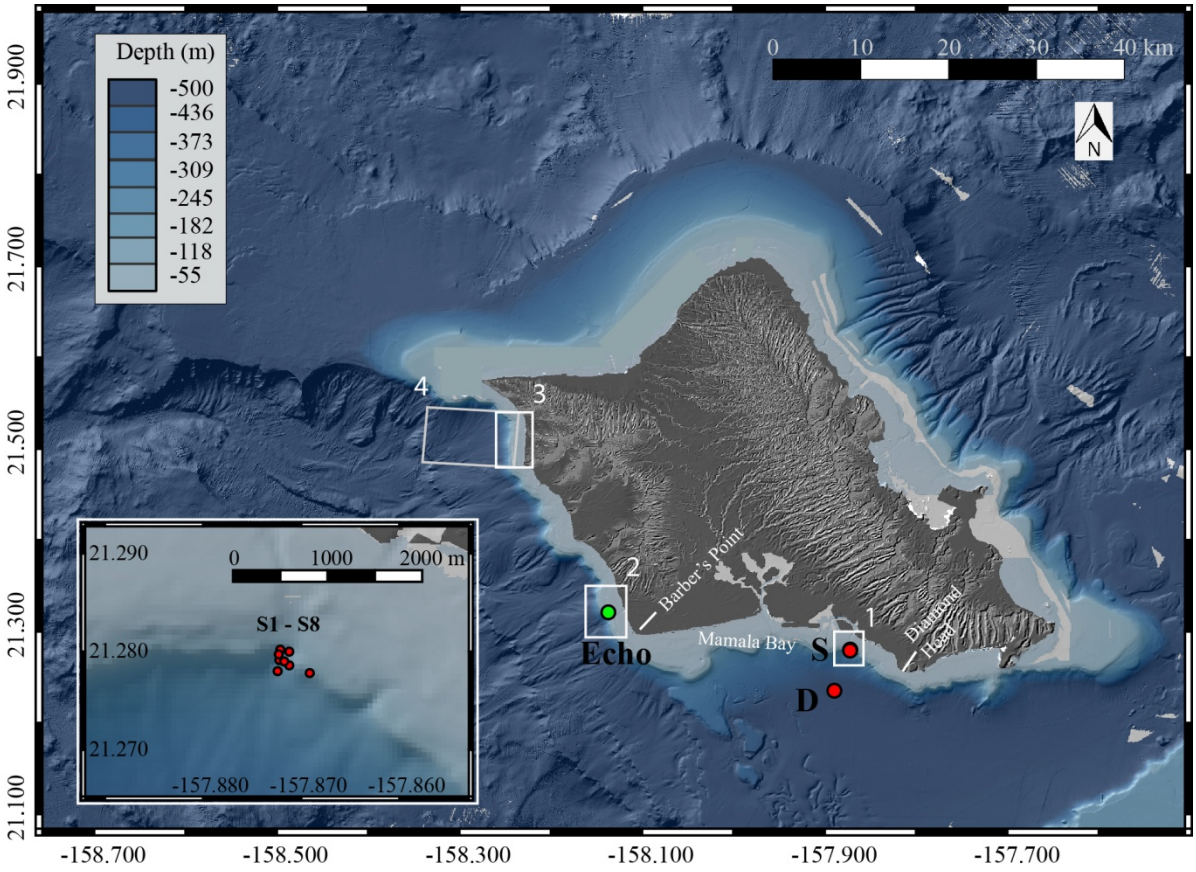

Figure 1. Map of the study location off the island of Oahu, HI. The shallow and deep deployments reported in this study are shown as circles labeled "S" and "D". Box 1 is enlarged in the inset and shows a close-up of the locations of the eight shallow deployments (S1–S8). The circle in box 2, labeled "Echo," shows the location of a 200 kHz echosounder and 300 kHz ADCP deployed in 2005 in a separate study and used here for method validation purposes [15]. Areas where the mesopelagic boundary layer and plankton layer dynamics have been previously studied are indicated by box 2 [15], box 3 [9], and box 4 [15–19].

2.3. General flow patterns

Previous work has described the general flow at the shallow site. When integrated throughout the water column, flow is typically higher in the alongshore direction, but near the benthos bathymetric steering of a small canyon drives a dominant across-shore current [20]. The current flow direction primarily varies at the time scale of the M_2 tidal constituent throughout the water column, including near the benthos [20]. The M_2 constituent is the principal lunar semidiurnal tide, which has a period of 12.42 h and is the dominant tidal constituent in most of the world's oceans. At both shallow and deep sites, the alongshore and across-shore velocities were calculated based on the major and minor axes for each deployment. The major axes of the current ellipses ranged from 103–119, which correspond to an alongshore direction. The depth-integrated alongshore and across-shore flow components were calculated for the full range of ADCP data and for the near-bottom portion of the water column (8–16 meters above bottom). Mean current magnitudes in the across-shore direction were compared to calculated community movement speeds to ascertain the possible impact of advection on the observed migratory phenomenon.

2.4. Backscatter estimation and general calculations

The acoustic volume scattering strength (S_v, dB re 1 m^{-1}), or backscatter, was estimated from ADCP echo intensity data following the methods of [21]. Geometric means and standard deviations were used because the data are on a logarithmic scale. The geometric means and geometric standard deviations of estimated backscatter data were calculated for each deployment during daytime and nighttime periods. Daytime was defined as the time between local sunrise and sunset, and nighttime was defined as the time between local sunset and sunrise. Sunrise and sunset data for Honolulu, HI were obtained from the U.S. Naval Observatory (http://aa.usno.navy.mil).

The ADCPs in this study were deployed with the primary goal of investigating flow and were not calibrated to allow derivation of absolute backscatter strength, in contrast to a previous study on Oahu [22]. Therefore, all backscatter (S_v) values reported here are estimated, and they should not be directly compared between sites or instruments. However, the important factor in identifying micronekton diel migration is the relative change in estimated backscatter over time at each individual ADCP; therefore, when comparing two deployments, the estimated backscatter was normalized on a 0–1 scale, with 0 being the lowest estimated backscatter and 1 being the highest estimated backscatter within the time frame of interest.

2.5. Identifying migrations using diel changes in estimated backscatter

The mesopelagic boundary layer moves between deep (~400–600 m) and shallow (0–400 m) waters along the slope during the diel migrations [9]. In a full diel migration cycle, there is an evening arrival at the shallow habitat, a morning departure from the shallow habitat, a morning arrival at the deep habitat, and an evening departure from the deep habitat. The times of these events each day were

identified using changes in the estimated backscatter at the deep and shallow ADCPs, and the community movement speed was estimated using departure and arrival times at deep and shallow moorings during the evening migration. It is important to note that the same *individuals* may not be detected at both ADCP sites, despite their positioning as an across-shore transect; however, the *community* as a whole leaves a deep habitat and migrates to a shallower habitat, so we can use these two instruments to estimate community arrival and departure times and community movement speeds between ~520 m and ~100–150 m isobaths. We do not attempt to resolve individual swimming speeds.

We focused on the deepest part of the water column at each site, corresponding to a range of 8–16 m above the benthos, where the daily variation in backscatter was most pronounced (Figure 2). The mean of estimated backscatter was taken over this depth range at each time point to produce a single time-series of estimated backscatter, and the time-series was then filtered using a 1-hour low-pass Butterworth filter to remove high-frequency variation. Using this filtered time-series, we calculated the mean estimated backscatter for each non-migration period (day and night). For the shallow sites, the "non-migration periods" were defined as 00:00–02:00 and 10:00–18:00, based on previous observations of the community behavior in a shallow nighttime habitat in Hawaii's waters [15]. For the deep site, published observations were not available, and so the non-migration periods were defined as 01:00–04:00 and 10:00–15:00 based on observed patterns in the backscatter time series.

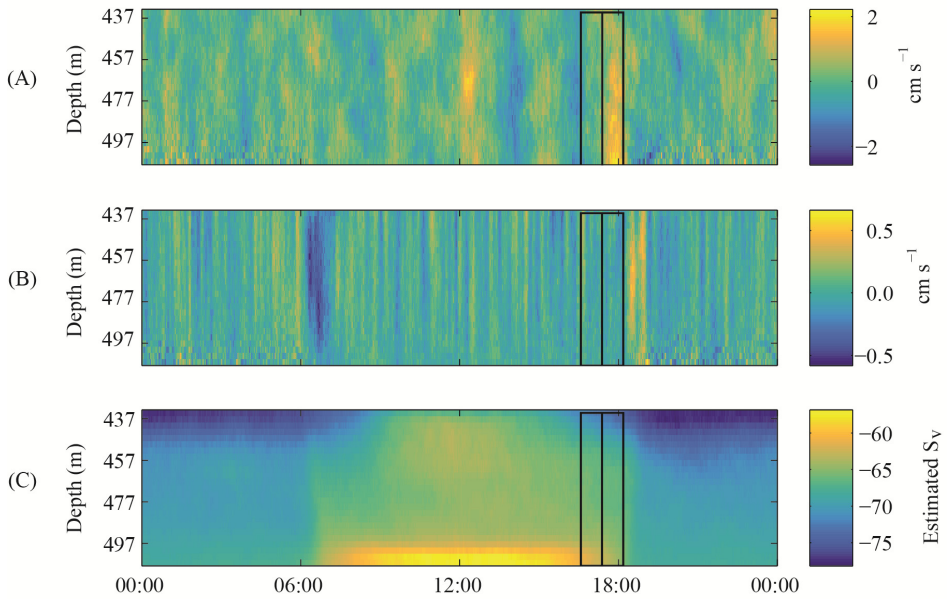

Figure 2. Sample mean-day composites for March 3–May 2, 2013 at the deep site. (A) High-pass filtered cross-shore velocity, (B) high-pass filtered vertical velocity, (C) estimated backscatter. The intersection of the two black rectangles represents the mean time of departure from deep site, and the boundaries of the rectangles represent one standard deviation. Note the difference in scale between A and B.

Each migration event was then bounded by a "high" and "low" estimated backscatter mean. We estimated the times of daily migration events by identifying when the estimated backscatter signal rose or fell past certain percentage thresholds between consecutive low and high periods. We used a 50% threshold for statistical analyses (midway between day and night average backscatter readings), and used 20% and 80% thresholds to visualize the time-span over which migrations occurred. The times that the thresholds are crossed are referred to as the "arrival" and "departure" times of the community.

Most of the time, the change in estimated backscatter during the migration periods was clear and abrupt. However, sometimes the signal was noisy or sloped slowly, which resulted in reduced confidence in the identification of the migration time. To control for this, the slopes of the filtered data for the one hour surrounding the identified migration times were calculated for each day. The observations associated with the lowest 20^{th} percentile of slopes were removed from analysis.

2.6. Validation: Relating ADCP observations to mesopelagic boundary community migration

To provide confidence that observed changes in estimated backscatter were associated with the diel migration of the mesopelagic boundary layer, we examined data from two instruments deployed simultaneously [15]. One instrument was a 200 kHz echosounder calibrated to observe the presence of myctophid fishes [14], and the second was a 300 kHz ADCP. The instruments were deployed together at 40 m water depth off the southwest side of Oahu during April 2005 (Figure 1) [15]. By applying the method described in section 2.5 to the 2005 ADCP data, we found that estimated dusk arrival times ranged from 18:15–20:42. The echosounder recorded arrival times of 18:15–21:00. Estimated dawn departure times using the ADCP data were 4:54–7:00, but the echosounder showed that the departure actually happened between 02:15–4:30.

At the deep site, the diel change in the near-bottom backscatter signal could be due to migration to a shallower pelagic habitat (vertical), slope-associated migration that moves inshore and shallower at night (horizontal), or both. We explored the data for evidence of horizontal and vertical components of the migration by examining "mean-day" composites of vertical and cross-shore velocities at the deep site [23]. ADCPs determine water velocity by measuring the velocity of suspended sound-scattering particles in the water column, such as sediment and plankton. These velocity measurements can be biased by nektonic organisms swimming through the water rather than being advected [23,24]. If a large-scale migration in a unified direction occurs at a certain time each day, these animal movements can manifest as a noticeable signal in a mean-day composite [23]. In the mean-day analysis, velocity data were first filtered with a 4^{th}-order high-pass Butterworth filter to remove changes occurring with periods greater than 5 hours. This was done to remove bias in the means due to tidal effects.

Distinct vertical and horizontal signals were visible in mean-day visualizations of filtered data (Figure 2). The mean-day composite of vertical velocity showed a short period of downward velocity centered near 06:30 and a short period of upward velocity centered near 19:00. The mean-day composite of cross-shore velocity showed a period of shoreward velocity centered slightly earlier than 18:00, concentrated mainly in the bottom 30 m. The shoreward pulse corresponded to the period of time and depth where estimated backscatter was decreasing. These results support the assertion that the daily fluctuations in the near-bottom estimated backscatter were significantly due to the presence/absence of the horizontally migrating micronekton community. Note that there was no significant offshore velocity in the morning that would correspond to a horizontal return to deep water. This observation indicates that the horizontal morning migration was less concentrated in time than the horizontal evening migration.

Since the algorithm was more accurate for the dusk event than the dawn event, and the mean-day composites also showed a stronger signal at dusk than at dawn, we focused primarily on the dusk migration for statistical modeling and other analyses.

2.7. Generalized additive modeling

We tested the hypothesis that evening arrival time of the mesopelagic boundary community at the shallow site varied with sunset time, lunar illumination, cloud cover, and water column depth. Lunar illumination was defined as the percent of moon illuminated if the moon was up in the sky, but if the moon was not up between sunset and the arrival time or set/rose within one hour of arrival time (meaning moon was low on the horizon), the illumination was set to zero. Sun and moon data were obtained from the US Naval Observatory (http://aa.usno.navy.mil). Cloud cover was the mean percentage of the sky covered in clouds for each evening (18:00–00:00). Cloud data were obtained from the National Climate Data Center's Honolulu International Airport station at one hour intervals (http://www.ncdc.noaa.gov).

Arrival times of the mesopelagic boundary layer at the shallow site were hypothesized to be due to environmental factors, namely sunset, cloud cover, lunar illumination, and water column depth. We employed a generalized additive model (GAM) to model this research hypothesis, as the error distribution of our response (and thus likely our residuals) was non-normal (approximately gamma) and relationships between response and predictor variables were assumed to be non-linear. The inverse (vs. log) link function resulted in the best-behaved residuals. Co-linearity among predictors was assessed both by calculating Pearson's correlation values and variance inflation factors (VIF, for multicollinearity) [25]. Correlation among predictors was found to be low (i.e., all VIFs < 3) [25] and all predictors were maintained in the model fit. Model selection continued by comparing models representing all possible combinations of predictors. The best-specified model was chosen based on corrected Akaike information criterion (AICc) and comparisons of model complexity (number of predictors). In

addition, the assumption of non-linear relationships was tested by refitting the model with a Generalized Linear Model (GLM, with inverse link function) including main effects and all-way interactions of the predictor variables.

Statistical modeling was performed in R [26] using the mcgv, car, AICcmodavg, and MuMIn packages [27–30]. Other calculations were performed in MATLAB [31].

3. Results

3.1. General flow patterns

In general, the current magnitude in the alongshore direction was greater than the current magnitude in the across-shore direction, and the current magnitudes at the deep site were higher than the current magnitudes at the shallow site (Table 2; Figure 3). However, in the bottom layer of the shallow site (8–16 m above bottom), we observed higher magnitudes in the across-shore direction than the alongshore direction (Table 2; Figure 3). Variation in alongshore and across-shore velocities were a function of the M_2 tidal constituent (12.42 h) and centered around zero, meaning that when organisms migrated upslope and downslope, they sometimes swam with the current and sometimes against it.

Table 2. Measured current magnitudes in the alongshore and across-shore direction at shallow and deep sites.

	Mean current speed (cm s^{-1})		***Mean current magnitude (cm s^{-1})***	
8-16 m above seafloor	**Alongshore**	**Cross-shore**	**Alongshore**	**Cross-shore**
Shallow site	0 ± 4.46	0 ± 4.34	3.33 ± 2.97	4.75 ± 6.44
Deep site	0 ± 13.93	0 ± 7.54	10.98 ± 8.58	5.94 ± 4.65
Full ADCP range				
Shallow site	0 ± 5.93	0 ± 2.99	4.50 ± 3.85	2.29 ± 1.92
Deep site	0 ± 12.20	0 ± 5.05	9.67 ± 7.39	3.97 ± 3.12

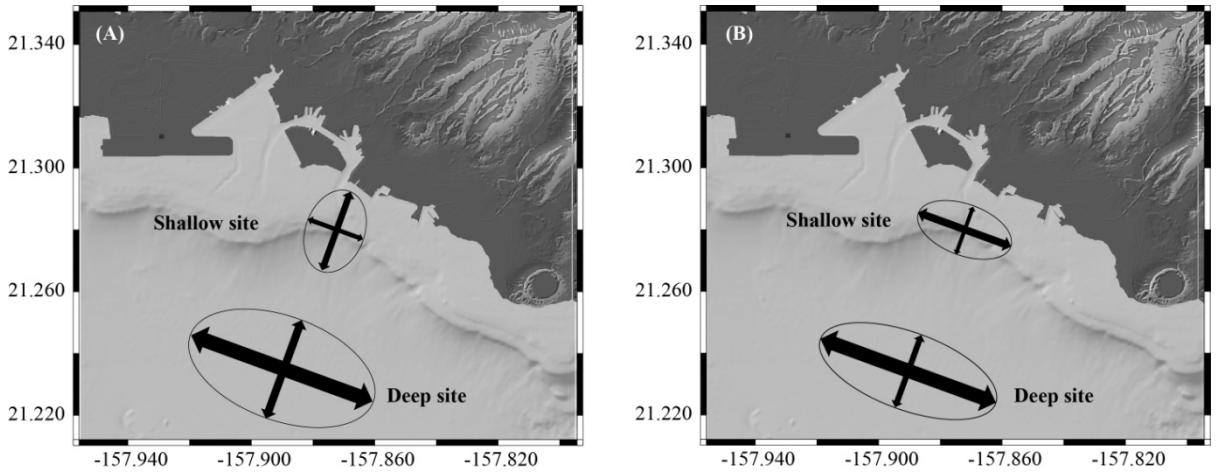

Figure 3. Visualizations of alongshore and across-shore current magnitudes. Arrow size represents the relative magnitude of the currents, all of which vary tidally around zero. (A) Visualization of currents observed at 8-16 m above the bottom. (B) Visualization of currents integrated throughout the full range of the ADCP (~100 m above bottom).

3.2. Estimated Acoustic Volume Scattering Strength (S_v): Results and observed patterns

Estimated S_v was calculated from echo intensity data for all ADCP deployments. For the six-month deployment of the deep ADCP (D), estimated S_v was typically higher during the day (-59.4 ± 1.1 dB) than at night (-68.1 ± 1.0 dB) (Table 3). In contrast, each of the shallow deployments had higher estimated S_v during the night than during the day (Table 3). Moorings S1 and D were deployed simultaneously and high estimated S_v occurred during the day at the deep site (D) and during the night at the shallow site (S1) (Figure 4).

Table 3. Estimated backscatter statistics for each deployment. ***Note: These ADCPs were not calibrated, so estimated backscatter should only be compared within deployments, not between deployments.*** **The same ADCP was used from deployments S4-S8.**

Estimated Backscatter (S_v) Statistics	*Day (geomean ± geostd)*	*Night (geomean ± geostd)*
		Mean
D	-59.4 ± 1.1	-68.1 ±1.0
S1	-64.0 ± 1.1	-52.8 ± 1.1
S2	-75.4 ± 1.0	-64.0 ± 1.1
S3	-69.4 ± 1.1	-58.6 ± 1.1
S4	-65.4 ± 1.1	-58.4 ± 1.1
S5	-68.0 ± 1.1	-58.5 ± 1.1
S6	-67.5 ± 1.1	-54.3 ± 1.1
S7	-62.2 ± 1.1	-54.6 ± 1.1
S8	-68.7 ± 1.1	-58.3 ± 1.1

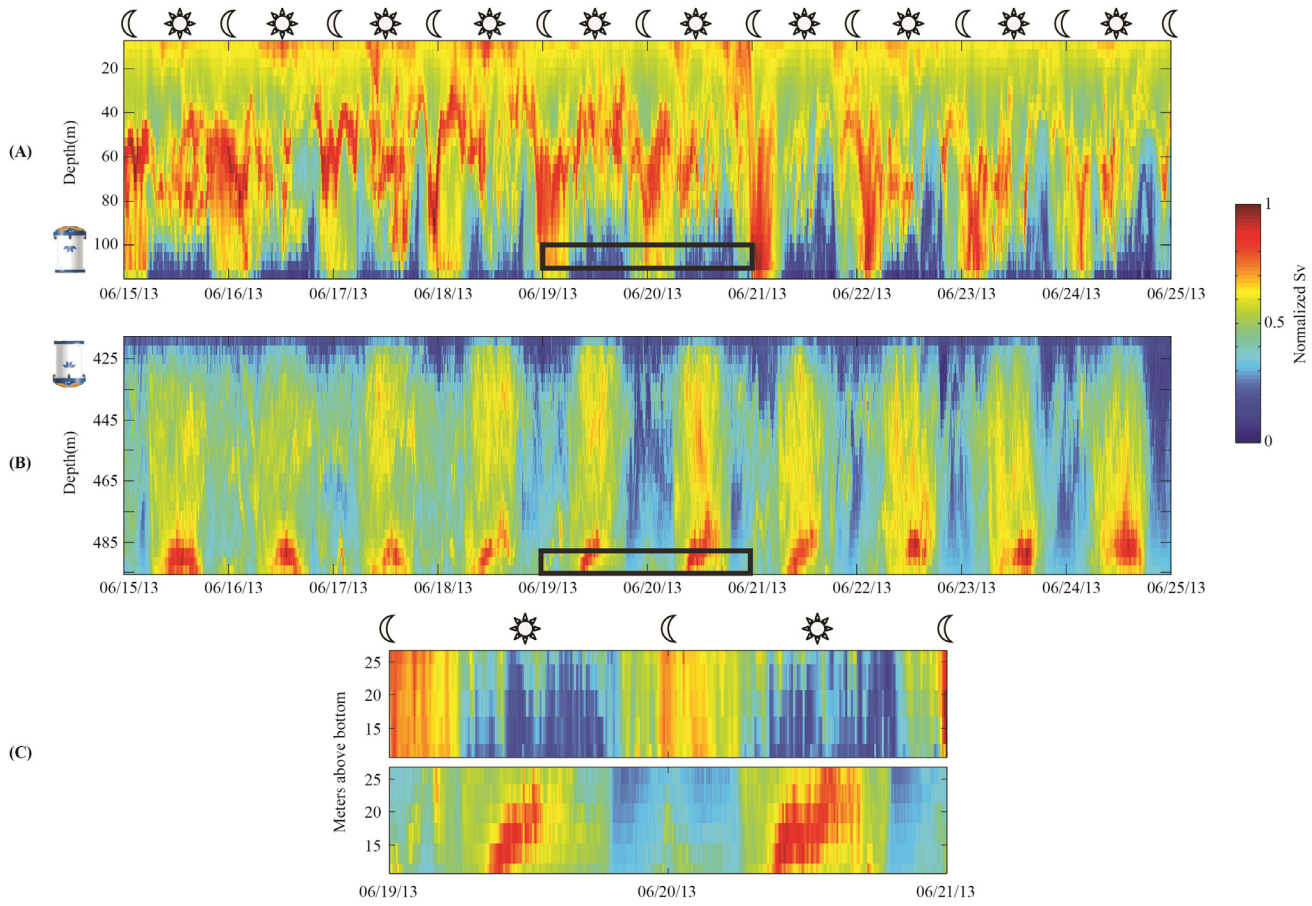

Figure 4. Contour plots of normalized estimated S_v (scale: 0–1) for a sample 10-day period. (A) Deployment S1 (bottom depth 120 m), where estimated backscatter was generally higher at night. (B) Deployment D (bottom depth 517 m), where estimated backscatter was generally higher during the day. (C) Close-up of the bottom layer for two days highlights the diel patterns (upper panel is from deployment S1; lower panel is from deployment D).

3.3. Arrivals and departures of the scattering community

Arrival and departure times relative to sunrise and sunset were calculated for each event in the diel cycle: arrival at the shallow site, departure from the shallow site, arrival at the deep site, and departure from the deep site. Estimated mean arrival time at the shallow site was 38 ± 57 min after sunset. Departure from the shallow site was 14 ± 89 min before sunrise. Arrival at the deep site was 54 ± 39 min after sunrise, and departure from the deep site was 81 ± 43 min prior to sunset (Figure 5).

Using the 20% threshold for departure from the deep site and the 80% threshold for arrival at the shallow site (that is, the time that the migration away from the deep site was beginning to the time that the arrival at the shallow site was nearly complete), the migration time was estimated to be 4 h 13 min ± 1 h 25 min. Using 50% departure and 50% arrival thresholds, the migration time was estimated to be 2 h 38 min ± 1 h 18 min. The deep and shallow ADCPs were located 5.25 km apart,

so assuming zero net cross-shore current, these elapsed time measurements correspond to estimated mean community movement speeds of 1.99 km h^{-1} (55 cm s^{-1}) using the 50% to 50% thresholds, or 1.25 km h^{-1} (35 cm s^{-1}) using the 20% to 80% thresholds. However, we did measure cross-shore current velocities, and 95% of cross-shore current velocity measurements in the water column were less than 10.1 cm s^{-1} (Table 2). Additionally, the variability in cross-shore current direction occurs at an M2 tidal frequency, so different days would have different current directions during the migration time frame. Therefore, we show that this observed migration was not driven solely by advection, but more likely by swimming organisms, as was observed by [15].

The speeds of the shoreward and vertical signals shown in the mean-day plots are much slower (0.5–2.0 cm s^{-1}), but these signals should only be interpreted as directional indicators. The values result from averaging both over two-minute intervals as recorded by the ADCP and over many days for the mean-day composite, during which current speeds near zero were also often observed. Therefore, the mean-day velocities can be expected to be lower than actual micronekton swimming speeds.

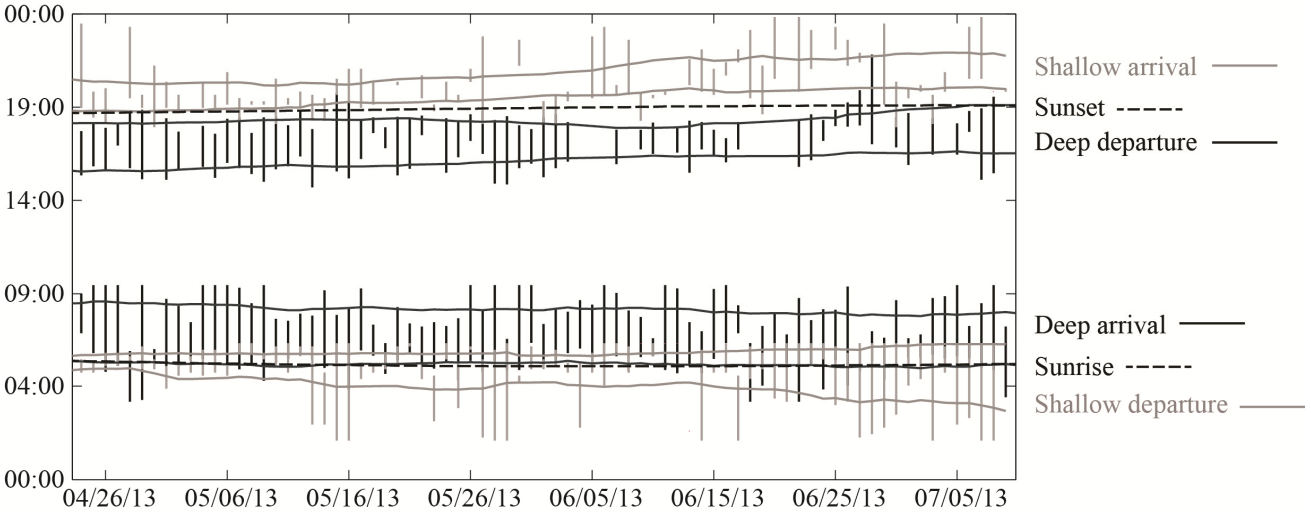

Figure 5. Departure and arrival times calculated from the D (black) and S1 (grey) deployments, shown for the span of time when deep and shallow instruments were simultaneously deployed. The vertical lines span the 20% to 80% thresholds for departures and arrivals, and the horizontal black lines represent a running mean of the deep sensor results (20% and 80%.) The horizontal grey lines represent a running means of the shallow sensor results (20 and 80%). The dashed lines indicate sunrise and sunset times.

3.4. Statistical modeling

The best-specified GAM (assessed via corrected Akaike information criterion, AICc and number of predictors) included smoothed (non-linear) effects of sunset and lunar illumination. This GAM performed better than a GLM with predictors of sunset and lunar illuminations and their interaction

(based on AICc; -1855 and -1869 respectively) and the GAM was chosen as the best-specified model. The GAM was significant (P << 0.0001), explaining 39.3% of the deviance in the time of arrival. Sunset time explained 36.6% of the deviance, and the addition of lunar illumination to the model explained an additional 2.7%. The GAM model prediction is plotted over a scatterplot of sunset time versus arrival time in Figure 6.

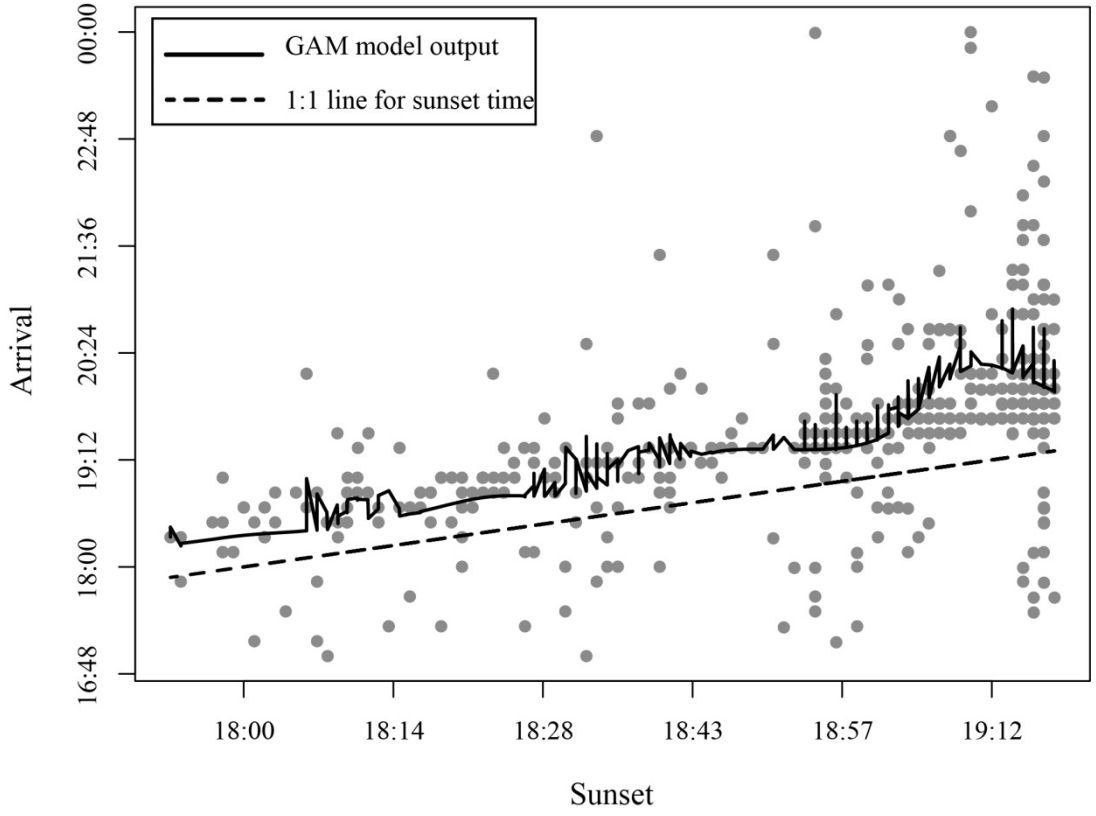

Figure 6. Arrival plotted as a function of sunset time. The dashed line is the 1:1 line for sunset time. The solid black line represents the predicted values of the best-fit GAM. The jagged fluctuations in the prediction line are due to lunar illumination, which was included in the model but is not on the plot axes.

4. Discussion

The mesopelagic boundary community in Hawaii has been previously studied using a variety of methods, including net tows [7], stereo-video cameras and standard video [9], and calibrated echosounders [9,14–16,19]. Many of these studies have taken place along the western coasts of Oahu and the Big Island of Hawaii. This study contributes to this growing body of literature by being the first to observe the full diel migration of the mesopelagic boundary community on the southern slope of Oahu from departure to arrival and back again. This study is also unique in that it

uses long-term moorings at both shallow and deep habitats to better assess the effects of changing seasons and lunar illumination on micronekton behavior.

4.1. Extraction of useful biological data from a physical oceanographic instrument

Data collected with the uncalibrated ADCPs in this study were able to reveal valuable observations about the behavior of the community of scattering organisms known as the Hawaiian mesopelagic boundary community. Through our comparison of a calibrated 200 kHz echosounder and uncalibrated 300 kHz ADCP data from a 2005 deployment [15], we showed that uncalibrated 300 kHz ADCP data could be used to estimate the behavior of the mesopelagic boundary layer community via changes in estimated backscatter readings, particularly during the evening migration. Though calibrated echosounders and/or calibrated acoustic Doppler current profiles (ADCPs) would provide more refined data [14,32], valuable biological information was successfully extracted from uncalibrated ADCP data even though the deployments were designed for measuring ocean currents rather than biological signals. This analysis enabled us to maximize the usefulness of the ADCP data collected at these sites by observing patterns in micronekton behavior in addition to the intended observations of the current field.

While many factors can affect the observed echo intensity (and therefore the estimated backscatter) including turbulence, suspended solids, bubbles, and changes in plankton and micronekton density [33], the time scales of variability observed in these deployments further supports the assertion that these changes in backscatter are due to migrating organisms. Some typical sources of variability in estimated backscatter, such as sediment suspension and turbulence, would be more likely to vary at tidal scales rather than a daily scale. There would be no mechanistic reason for sediment suspension or turbulence to vary on diel frequencies at > 100 m depth in the water column in Hawaii. Diel variability in estimated backscatter at these depths is much more likely to be related to the diel habitat shifts of mesopelagic scattering organisms.

4.2. General observations

The general flow and estimated backscatter patterns observed in this study are consistent with previous work. Flow on the south shore of Oahu is strongly influenced by internal tides [34], and the predominant flow direction is generally alongshore and tidally variable [20,35,36]. There was significant across-shore flow observed at the shallow moorings in the near-bottom layer, which is likely caused by bathymetric steering due to the moorings' location in a submerged channel [20].

We observed higher estimated backscatter readings at night in shallow water and during the day in deeper water. These patterns are consistent with the known diel vertical and horizontal migration of the scattering community along the Oahu slope [7,14,32]. Additionally,

the across-shore currents measured were lower than the movement speeds calculated for the mesopelagic boundary community and were sometimes flowing opposite the direction of movement, supporting previous observations that showed swimming behavior to be more important than current advection [15]. The unique discoveries from this work are summarized in the following sections.

4.3. Environmental drivers of the timing of migration

Changes in estimated backscatter readings over time allowed estimation of mesopelagic boundary community arrivals and departures at both shallow and deep sites, though this method was found to be more reliable during the evening migration than the morning migration. At the shallow site, the evening arrival time of the mesopelagic boundary community was correlated with sunset time and lunar illumination.

Previous research on western Oahu showed no correlation between the onset of mesopelagic boundary community migration and sunset time [15]. In [15], moorings were deployed at 10–40 m depth, but due to the relatively short length of the deployments (~35 days), the sunset time only varied by 15 minutes. In the current study, 80–100 day deployments in multiple seasons resulted in higher variability in sunset time, spanning about 70 minutes. The greater variation in sunset time may have allowed this correlation to emerge from a variable data set where a host of other factors potentially influence micronekton behavior and estimated backscatter readings.

Moon phase has previously been shown to have a significant positive correlation with arrival time at moorings in 10–40 m water depth [15]. In this study, we found that night sky brightness was a significant factor influencing the dusk arrival time, as measured by the percent of the moon illuminated in the sky. The deviance explained by the GAM (39.3%) indicates that other sources of variability exist. *In situ* surface irradiance measurements and light at depth measurements were not available in this study, but may be important explanatory factors for variability in micronekton behavior. Changes in backscatter could also be caused by physical processes such as tidal flow, eddies, and internal waves, thin layers of phytoplankton and zooplankton [16,19], or suspended sediment.

The observations of later arrivals of the scattering community with later sunset times and brighter night skies indicate that the community is likely responding to proximate light cues in the environment. The competing interests of avoiding visual predators and foraging drive diel migrations in zooplankton and micronekton species in locations throughout the world [12,37–43]. In open ocean environments, the timing of diel vertical migration and depths of residence of zooplankton and micronekton scattering layers have been shown to be closely related to changing light levels, while other factors such as dissolved oxygen concentration are less important [6,43,44]. The moon phase has also been shown to influence the nighttime distribution of slope and

seamount-associated micronekton [45,46]. Light changes unrelated to daily or lunar cycles also affect the behavior of pelagic micronekton. In a high-latitude environment, myctophid fishes increased their daytime residence depth and began to school (presumably as a predator avoidance mechanism) during lit summer nights [47], and pelagic crustaceans and gelatinous zooplankton were observed decreasing their depth by about 100 m during a daytime influx of turbid water [48]. Our observations of the migration of the slope-associated micronekton community on Oahu, HI align with these observations and continue to support light-based mediation of micronekton diel migrations and residence depths, both in the pelagic and in slope-associated habitats.

The timing of the dawn downslope migration was variable and the onset of events was less defined in nature compared to that of the evening upslope migration. Migrating organisms may forage in the shallower, relatively food-rich environment until they are satiated and then begin their downslope migration well before any dawn light cues become apparent [40,49]. We also suggest that predation pressure could disperse the foraging community and drive individual organisms to depth throughout the nighttime period. This more gradual descent may have contributed to the uncertainty in identifying the dawn migration time using estimated backscatter data.

4.4. Migration and swimming speed

Micronekton on the Oahu slope have been previously shown to migrate between 5.5 and 11 km round-trip each day as part of their diel migration [9]. Assuming that the horizontal migrators observed at the deep site in this study were also detected at the shallow site, the micronekton community was undertaking diel migrations of at least 10.6 km (twice the distance between the deep and shallow mooring sites) and up to ~14 km if they continued to shallower depths nearer to shore. Estimated community movement speeds from this work ranged from 1.25–1.99 km h^{-1} (35–55 cm s^{-1}). Previously observed swimming speeds of myctophids ranged from 0.4–2.8 km h^{-1} (11–78 cm s^{-1}) [7,50], and previous studies of the mesopelagic boundary community on Oahu reported horizontal swimming speeds of 0.9 km h^{-1} (25 cm s^{-1}) [32] to 1.8 km h^{-1} (50 cm s^{-1}) [15]. Therefore, the community movement speed estimated here does align with previously observed myctophid swimming speeds.

4.5. Ecological importance and vulnerability to a marine industrial development

The mesopelagic boundary community is an important component of the Hawaiian slope ecosystem, as members of the community consume large quantities of copepods and euphausiids in Hawaii's near-shore waters [51]. Mesopelagic micronekton are also a primary food source for higher trophic level predators such as spinner dolphins *Stenella longirostris* [10] and large pelagic fishes such as bigeye tuna *Thunnus obesus* and swordfish *Xiphias gladius* [52,53].

New coastal development may soon impact the Hawaiian mesopelagic boundary community on the southern slope of Oahu. A seawater air conditioning (SWAC) system is proposed for the

area of this study. The SWAC system will pipe deep, cold ocean water from 500 m depth and use the cold water in a heat-exchange system to cool a freshwater loop, which will then be piped to the downtown business district to use as air conditioning coolant [54]. The warmed deep seawater will then be discharged via a diffuser spanning 100–140 m depth along the slope. The discharged water will have a higher concentration of nutrients and lower oxygen concentration compared to the ambient water, among other differences [20,54], which may result in local increases in phytoplankton production. Higher productivity and gradients in temperature, density, salinity, and oxygen associated with the plume may cause attraction or avoidance of mesopelagic fishes [55].

Light penetration to depth is likely to be very important in driving mesopelagic boundary community migrations, and water column clarity may be affected by eutrophication from industrial operations like the proposed seawater air conditioning plant or future development of ocean thermal energy conversion, a similar technology based on artificial upwelling [56]. Changes in water clarity and the rate of light extinction with depth have the potential to influence the diel migratory patterns of both pelagic and slope-associated organisms, which may in turn lead to ecosystem impacts including changes in the transfer of nutrients between shallow and deep habitats and in the foraging patterns of predators. Additionally, the discharge will be into the pycnocline, which may cause spreading of the plume over a larger horizontal area and expand the geographic scale of any impacts [20].

Entrainment of organisms is another potential impact of the SWAC system on the mesopelagic boundary community. The intake site of the SWAC pipe will be located near the benthos at 500 m depth, where we observed both vertical and horizontal diel migrators residing during the day. The uncalibrated estimated backscatter data reported in this study do not allow estimates of the density of organisms, but high densities of micronekton in this environment are certainly possible. Submersible dives on other slope environments have revealed persistent and very dense aggregations of micronekton between 0–20 m from the benthos [57], and maximum observed densities of the mesopelagic boundary community in Hawaiian waters can exceed 1000 animals m^{-3}, although mean densities are much lower [14]. The intake velocity of the deep pipe will be 5.47 km h^{-1} (152 cm s^{-1}). Burst swim speeds of Hawaiian myctophid fishes are not specifically known. If the burst speeds are lower than the flow rate, they will be at high risk of entrainment, and even if burst swim speeds exceed the intake flow rate some members of the community will be entrained. Mesopelagic shrimp have burst swim speeds of only 0.72 km hr^{-1} (20 cm s^{-1}) [58]. Mortality rates associated with entrainment are not known, but it is likely that at least some organisms entrained in the flow will not survive the rapid temperature and pressure changes as they move through the system [59]. This will result in daytime deposition of deceased micronekton around the area of the diffuser system. Especially considering the potential high densities of micronekton at the SWAC intake site, entrainment and deposition could have a significant effect on the local benthic food web and be an additional food source for scavenging organisms.

5. Conclusions

The mesopelagic boundary community in Hawaii undertakes diel horizontal migrations that are driven by competing interests of foraging and predator avoidance. This study contributes to this growing body of literature by observing the full diel migration of the mesopelagic boundary community, from departure to arrival in both directions, on the southern slope of Oahu and by using long-term moorings at both shallow and deep habitats to better assess the effects of changing seasons and lunar illumination on micronekton behavior. The amount of ambient light plays a significant role in the timing of the migration, with later sunsets and brighter night skies corresponding to later arrival times of the mesopelagic boundary community in the food-rich shallow nighttime habitat. Even using uncalibrated estimated backscatter data, these patterns were observable and statistically significant. In light of increasing coastal development worldwide, it is important to understand how the slope habitat is being used by important intermediate trophic level organisms such as this migrating community. The enhanced understanding of the behavior of boundary layer organisms at this location will enable better assessment of anthropogenic impacts on this community and on the ecosystem as a whole.

Acknowledgments

Funding for this work was provided by the Office of Naval Research (Award number N0001414100054–Asia-Pacific Research Initiative for Sustainable Energy Systems (APRISES)), the State of Hawaii, the Joint Institute for Marine and Atmospheric Research, and the Office of the Dean of the School of Ocean and Earth Science and Technology. We would like to thank the following people for assistance with fieldwork and instrumentation: Douglas Luther, Mark Merrifield, Carly Quisenberry, Chris Kontoes, Gordon Walker, Sarah Searson, Conor Jerolman, and Paula Moehlencamp. We thank the University of Hawaii Marine Center, Parker Marine Corp., and Sea Engineering Inc. for vessel support.

Conflict of interest

Both authors declare no conflicts of interest in this paper.

References

1. Clarke TA (1973) Some aspects of the ecology of lanternfishes (Myctophidae) in the Pacific Ocean near Hawaii. *Fish Bull* 71: 403-434.
2. Gal G, Loew ER, Rudstam LG, et al. (1999) Light and diel vertical migration: spectral sensitivity and light avoidance by *Mysis relicta*. *Can J Fish Aquat Sci* 56: 311-322.

3. Bianchi D, Mislan K (2016) Global patterns of diel vertical migration times and velocities from acoustic data. *Limnol Oceanogr* 61: 353-364.
4. Tarling GA, Cuzin-Roudy J, Buchholz F (1999) Vertical migration behaviour in the northern krill *Meganyctiphanes norvegica* is influenced by moult and reproductive processes. *Mar Ecol-Prog Ser* 190: 253-262.
5. Salvanes AGV, Kristofersen JB. (2001) Mesopelagic fishes. *Encycl Ocean Sci* 1711-1717.
6. Staby A, Aksnes DL (2011) Follow the light-diurnal and seasonal variations in vertical distribution of the mesopelagic fish *Maurolicus muelleri*. *Mar Ecol – Prog Ser* 422: 265-273 .
7. Reid SB, Hirota J, Young RE, et al. (1991) Mesopelagic-boundary community in Hawaii: Micronekton at the interface between neritic and oceanic ecosystems. *Mar Biol* 109: 427-440.
8. Porteiro FM, Sutton T (2007) Midwater fish assemblages and seamounts. Seamounts: Ecology, Fisheries, and Conservation 12: 101-116.
9. Benoit-Bird KJ, Au WWL (2006) Extreme diel horizontal migrations by a tropical nearshore resident micronekton community. *Marine Ecology-Progress Series* 319: 1-14.
10. Benoit-Bird KJ, Au WW (2003) Prey dynamics affect foraging by a pelagic predator (*Stenella longirostris*) over a range of spatial and temporal scales. *Behav Ecol Sociobiol* 53: 364-373.
11. Hays GC (1995) Ontogenetic and seasonal variation in the diel vertical migration of the copepods *Metridia lucens* and *Metridia longa*. *Limnol oceanog* 40: 1461-1465.
12. Hays GC (2003) A review of the adaptive significance and ecosystem consequences of zooplankton diel vertical migrations. In: Migrations and dispersal of marine organisms. Springer Netherlands, 503: 163-170.
13. Prihartato PK, Aksnes DL, Kaartvedt S (2015) Seasonal patterns in the nocturnal distribution and behavior of the mesopelagic fish *Maurolicus muelleri* at high latitudes. *Mar Ecol-Progs Ser* 521: 189-200.
14. Benoit-Bird KJ, Au WW (2004) Diel migration dynamics of an island-associated sound-scattering layer. *Deep Sea Res Part I* 51: 707-719.
15. McManus MA, Benoit-Bird KJ, Woodson CB (2008) Behavior exceeds physical forcing in the diel horizontal migration of the midwater sound-scattering layer in Hawaiian waters. *Mar Ecol-Prog Ser* 365: 91-101.
16. Benoit-Bird KJ, McManus MA (2012) Bottom-up regulation of a pelagic community through spatial aggregations. *Biol lett* 8: 813-816.
17. McManus MA, Sevadjian JC, Benoit-Bird KJ, et al. (2012) Observations of thin layers in coastal Hawaiian waters. *Estuaries Coasts* 35: 1119-1127.
18. Sevadjian J, McManus M, Benoit-Bird K, et al. (2012) Shoreward advection of phytoplankton and vertical re-distribution of zooplankton by episodic near-bottom water pulses on an insular shelf: Oahu, Hawaii. *Cont Shelf Res* 50: 1-15.
19. Benoit-Bird KJ, McManus MA (2014) A critical time window for organismal interactions in a pelagic ecosystem. *PLoS ONE* 9: e97763.

20. Comfort CM, McManus MA, Clark SJ, et al. (2015) Environmental properties of coastal waters in Mamala bay, Oahu, Hawaii, at the future site of a seawater air conditioning outfall. *Oceanogr* 28: 230-239.
21. Deines KL (1999) Backscatter estimation using broadband acoustic Doppler current profilers. Current measurement. *Proc IEEE sixth working conf curr measurements* 249-253.
22. Sevadjian J, McManus M, Pawlak G (2010) Effects of physical structure and processes on thin zooplankton layers in Mamala Bay, Hawaii. *Mar Ecol - Prog Ser* 409: 95-106.
23. van Haren H (2007) Monthly periodicity in acoustic reflections and vertical motions in the deep ocean. *Geophys res lett* 34: 12.
24. Heywood KJ (1996) Diel vertical migration of zooplankton in the northeast Atlantic. *J Plankton Res* 18: 163-184.
25. Zuur AF, Ieno EN, Elphick CS (2010) A protocol for data exploration to avoid common statistical problems. *Methods Ecol Evolut* 1: 3-14.
26. R Core Team (2015) R: A language and environment for statistical computing. R Foundation for Statistical Computing, Vienna, Austria. https://www.R-project.org.
27. Wood SN (2011) Fast stable restricted maximum likelihood and marginal likelihood estimation of semiparametric generalized linear models. *J R Stat Soc* (B) 73: 3-36.
28. Fox J, Weisberg S (2011) An R companion to applied regression, Second edition, Sage, Thousand Oaks, CA.
29. Barton K (2015) Mumin: Multi-model inference. R package version 1151.
30. Mazerolle MJ (2015) Aiccmodavg: Model selection and multimodel inference based on (q) aic (c). R package version 20-3.
31. MATLAB version R2013a. (2013) The MathWorks Inc., Natick, Massachusetts.
32. Benoit-Bird KJ, Au WWL, Brainard RE, et al. (2001) Diel horizontal migration of the Hawaiian mesopelagic boundary community observed acoustically. *Mar Ecol-Prog Ser* 217: 1-14.
33. Clay CS, Medwin H (1977) Acoustical oceanography: principles and applications. Wiley. University of Michigan. 544.
34. Eich ML, Merrifield MA, Alford MH (2004) Structure and variability of semidiurnal internal tides in Mamala bay, Hawaii. *J Geophys Res: Oceans* 109: C5.
35. Hamilton P, Singer J, Waddell E (1995) Ocean current measurements. In: Mamala Bay Study Final Report 1. Project MB, 38 pp and appendices.
36. Alford MH, Gregg MC, Merrifield MA (2006) Structure, propagation, and mixing of energetic baroclinic tides in Mamala Bay, Oahu, Hawaii. *J Phys Oceanography* 36: 997-1018.
37. Clark CW, Levy DA (1988) Diel vertical migrations by juvenile sockeye salmon and the antipredation window. *Am Nat* 131: 271-290.
38. Bollens SM, Frost BW (1991) Diel vertical migration in zooplankton: Rapid individual response to predators. *J Plankton Res* 13: 1359-1365.

39. Lampert W (1993) Ultimate causes of diel vertical migration of zooplankton: New evidence for the predator-avoidance hypothesis. In: Diel vertical migration of zooplankton 79-88.
40. Ringelberg J (1995) Changes in light intensity and diel vertical migration: A comparison of marine and freshwater environments. *J Mar Biol Assoc U K* 75: 15-25.
41. Ringelberg J (1999) The photobehaviour of *Daphnia spp*. as a model to explain diel vertical migration in zooplankton. *Biol Rev* 74: 397-423.
42. Klevjer TA, Irigoien X, Røstad A, et al. (2016) Large scale patterns in vertical distribution and behaviour of mesopelagic scattering layers. *Sci Rep* 6: 19873.
43. Aksnes DL, Røstad A, Kaartvedt S, et al. (2017) Light penetration structures the deep acoustic scattering layers in the global ocean. *Sci Adv* 3: e1602468.
44. Gibson R, Atkinson R, Gordon J (2009) Zooplankton diel vertical migration—a review of proximate control. *Oceanography Mar Biol: Annu Rev* 47: 77-110.
45. Benoit-Bird KJ, Au WW, Wisdoma DW (2009) Nocturnal light and lunar cycle effects on diel migration of micronekton. *Limnol Oceanogr 54*: 1789-1800.
46. Drazen JC, Lisa G, Domokos R (2011) Micronekton abundance and biomass in Hawaiian waters as influenced by seamounts, eddies, and the moon. *Deep Sea Res Part I* 58: 557-566.
47. Kaartvedt S, Knutsen T, Holst JC (1998) Schooling of the vertically migrating mesopelagic fish *Maurolicus muelleri* in light summer nights. *Mar Ecol-Prog Ser* 170: 287-290.
48. Frank T, Widder E (2002) Effects of a decrease in downwelling irradiance on the daytime vertical distribution patterns of zooplankton and micronekton. *Mar Biol* 140: 1181-1193.
49. Pearre S (2003) Eat and run? The hunger/satiation hypothesis in vertical migration: history, evidence and consequences. *Biol Rev* 78: 1-79.
50. Torgersen T, Kaartvedt S (2001) In situ swimming behaviour of individual mesopelagic fish studied by split-beam echo target tracking. *ICES J of Mar Sci: J du Conseil* 58: 346-354.
51. Clarke TA (1980) Diets of fourteen species of vertically migrating mesopelagic fishes in Hawaiian waters. *Fish Bull* 78: 3.
52. Moteki M, Arai M, Tsuchiya K, et al. (2001) Composition of piscine prey in the diet of large pelagic fish in the eastern tropical Pacific ocean. *Fish Sci* 67: 1063-1074.
53. Holland KN, Grubbs RD (2008) Fish visitors to seamounts: Tunas and billfish at seamounts. In: Seamounts: Ecology, Fisheries & Conservation. Blackwell Publishing, Oxford, UK, pp 189-201.
54. Honolulu Seawater Air Conditioning LLC (2014) Final environmental impact statement for the proposed Honolulu Seawater Air Conditioning project, Honolulu, Hawai'i. In: Engineers USA Co (ed). Cardno TEC, Inc., Honolulu, HI, 834.
55. Comfort CM, Vega L (2011) Environmental assessment for ocean thermal energy conversion in Hawaii: Available data and a protocol for baseline monitoring. *OCEANS 2011 IEEE* 1-8.
56. Vega LA (2002) Ocean thermal energy conversion primer. *Mar Technol Soc J* 36: 25-35.
57. Gartner JV, Sulak KJ, Ross SW, et al. (2008) Persistent near-bottom aggregations of mesopelagic animals along the North Carolina and Virginia continental slopes. *Mar Biol* 153: 825-841.

58. Cowles DL (2001) Swimming speed and metabolic rate during routine swimming and simulated diel vertical migration of *Sergestes similis* in the laboratory. *Pac Sci* 55: 215-226.
59. Cunningham JJ, Magdol ZE, Kinner NE (2010) Ocean thermal energy conversion: Assessing potential physical, chemical, and biological impacts and risks. Coastal Response Research Center, University of New Hamphsire, Durham, NH, 33 pp and appendices.

AIMS Press